

pubs.acs.org/JACS Communication

Engineering a Blue Light Inducible SpyTag System (BLISS)

Emily J. Hartzell, Justin Terr, and Wilfred Chen*



Cite This: J. Am. Chem. Soc. 2021, 143, 8572–8577



ACCESS

Metrics & More





ABSTRACT: The SpyCatcher/SpyTag protein conjugation system has recently exploded in popularity due to its fast kinetics and high yield under biologically favorable conditions in both *in vitro* and intracellular settings. The utility of this system could be expanded by introducing the ability to spatially and temporally control the conjugation event. Taking inspiration from photoreceptor proteins in nature, we designed a method to integrate light dependency into the protein conjugation reaction. The light-oxygen-voltage domain 2 of *Avena sativa* (AsLOV2) undergoes a dramatic conformational change in its c-terminal Jα-helix in response to blue light. By inserting SpyTag into the different locations of the Jα-helix, we created a blue light inducible SpyTag system (BLISS). In this design, the SpyTag is blocked from reacting with the SpyCatcher in the dark, but upon irradiation with blue light, the Jα-helix of the AsLOV2 undocks to expose the SpyTag. We tested several insertion sites and characterized the kinetics. We found three variants with dynamic ranges over 15, which were active within different concentration ranges. These could be tuned using SpyCatcher variants with different reaction kinetics. Further, the reaction could be instantaneously quenched by removing light. We demonstrated the spatial aspect of this light control mechanism through photopatterning of two fluorescent proteins. This system offers opportunities for many other biofabrication and optogenetics applications.

Within the past decade, SpyCatcher/SpyTag has emerged as a powerful bioconjugation system for biofabrication and synthetic biology applications because of the ability to form a spontaneous isopeptide bond upon complementation. This reaction is efficient in a broad range of solution conditions, enabling rapid intracellular bioconjugation. Moreover, the SpyCatcher reaction is irreversible and has no sequence identity sensitivities when compared to sortase A- or intein-based approaches. While the original pair is capable of providing fast kinetics, variants have been engineered to improve the overall conjugation rate by up to 400-fold. Despite these attributes, conditional SpyTag/SpyCatcher pairs have not been reported to allow bioconjugation at the required spatial and temporal resolution.

Light is a valuable tool for fabrication as well as in the synthetic biology space. 9,10 Photoactivation can provide noninvasive, spatiotemporal control over reaction chemistries and cellular processes down to micrometer-scale resolution. 11,12 While light-sensitive chemistries have been used for the formation ^{13,14} and degradation ¹⁵ of hydrogels as well as patterning the capture and release of biomolecules, 14,16,17 most of these chemistries are not site-specific, resulting in a stochastic collection of protein orientations. Such uncontrolled functionalization often leads to protein unfolding and loss of activity. Other photochemistries require UV activation and are not compatible for eliciting cellular responses. In contrast, photoreceptors require only visible light to perform reversible assemblies,⁹ and these optogenetic photoreceptors are being exploited within biomaterials for the spatial and temporal control of mechanical properties and photopatterning.²⁴⁻²⁷ None of the current photoreceptor tools, however, can create irreversible covalent bonds on their own. While conditional split inteins have been used for light-responsive

conjugation,^{28,29} the low solubility of intein fusions makes them nonideal for biofabrication.

We intend to fill this gap by creating a synthetic photoreceptor to regulate the SpyCatcher/SpyTag conjugation (Figure 1A). The light oxygen voltage 2 domain from *Avena sativa* (AsLOV2) is particularly attractive.³⁰ It is smaller than other photoreceptors and can be functionally expressed in *E. coli.*³¹ Further, blue light induces unfolding of the C-terminal $J\alpha$ -helix, lending itself to the insertion of foreign peptides, which can be hidden in the folded, dark state.^{31–36}

The peptide insertion point within the J α -helix and mutations that affect caging and photocycle half-life can alter the degree of switching over a range of concentrations. ³¹ As the SpyCatcher/SpyTag isopeptide bond formation is irreversible, we took advantage of the highly blocked AsLOV2 iLID variant, ³⁴ which was shown to have tight blocking of the caged SsrA peptide to the SspB binding partner in the micromolar range, as a base for the insertion of SpyTag.

Peptides have been inserted as far in as residue 537; however, I539 is highly conserved and required for docking the J α -helix in the dark state. As the original SpyTag (ST) contains an isoleucine, we were able to create a 537 ST variant (Figure 1B). We additionally chose sites 540–544 for insertion of both ST and the kinetically faster SpyTag002 (ST002). To provide finer control over the dynamic range of switching, different combinations of a slower catcher $\Delta N_1 \Delta C_2$ (SC)³⁷

Received: March 25, 2021 Published: June 2, 2021





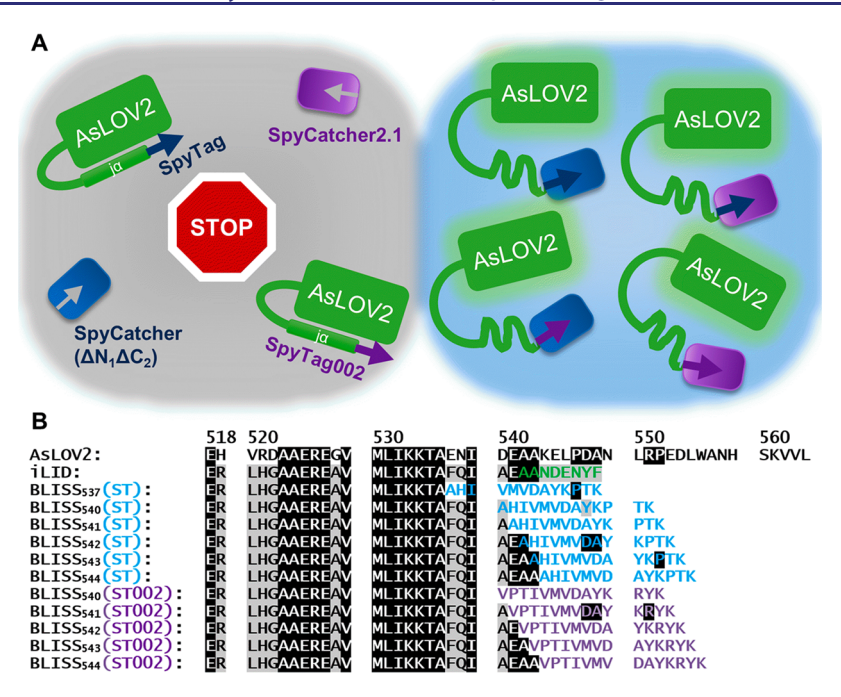


Figure 1. BLISS for conditional protein conjugation. (A) AsLOV2 variants with either SpyTag or SpyTag002 conditionally react with SpyCatcher($\Delta N_1 \Delta C_2$) or SpyCatcher2.1 to create tunable reaction kinetics. (B) BLISS variant C-terminal sequences aligned with AsLOV2 and iLID.³⁴ The black highlight identifies sequence similarities with AsLOV2, and the gray highlight identifies sequence similarities with iLID. The green text highlights the SsrA peptide in the iLID. The blue text highlights the SpyTag (ST). The purple text highlights SpyTag002 (ST002).

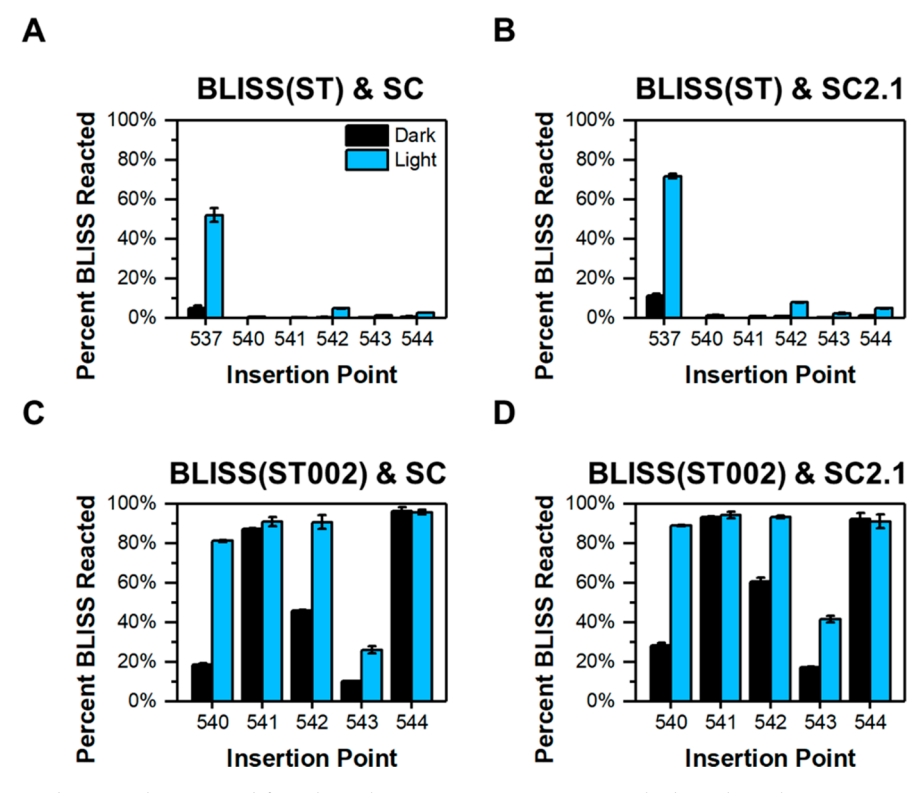


Figure 2. BLISS variants and SpyCatchers reacted for 1 h, each at 10 μ M concentrations. The bars show the average percent BLISS reacted with the standard deviation from three replicates shown as error bars. (A) BLISS(ST) variants reacted with SC. (B) BLISS(ST) variants reacted with SC2.1. (C) BLISS(ST002) variants reacted with SC2.1.

and a faster catcher, SpyCatcher2.1 (SC2.1)³⁸ with a slow tag (ST)³ and a faster tag (ST002)⁷ were evaluated (Figure 1A). All SpyCatcher constructs were expressed as C-terminal fusions to a Z-domain elastin-like polypetide (Z-ELP) biopolymer for simple purification.^{39,40}

The blue light inducible SpyTag system (BLISS) variants were initially evaluated at 10 μ M concentrations for 1 h to determine the best insertion locations (Figure 2 and S1). All the BLISS(ST) variants showed good blocking in the dark state; however, with the exception of 537, they showed

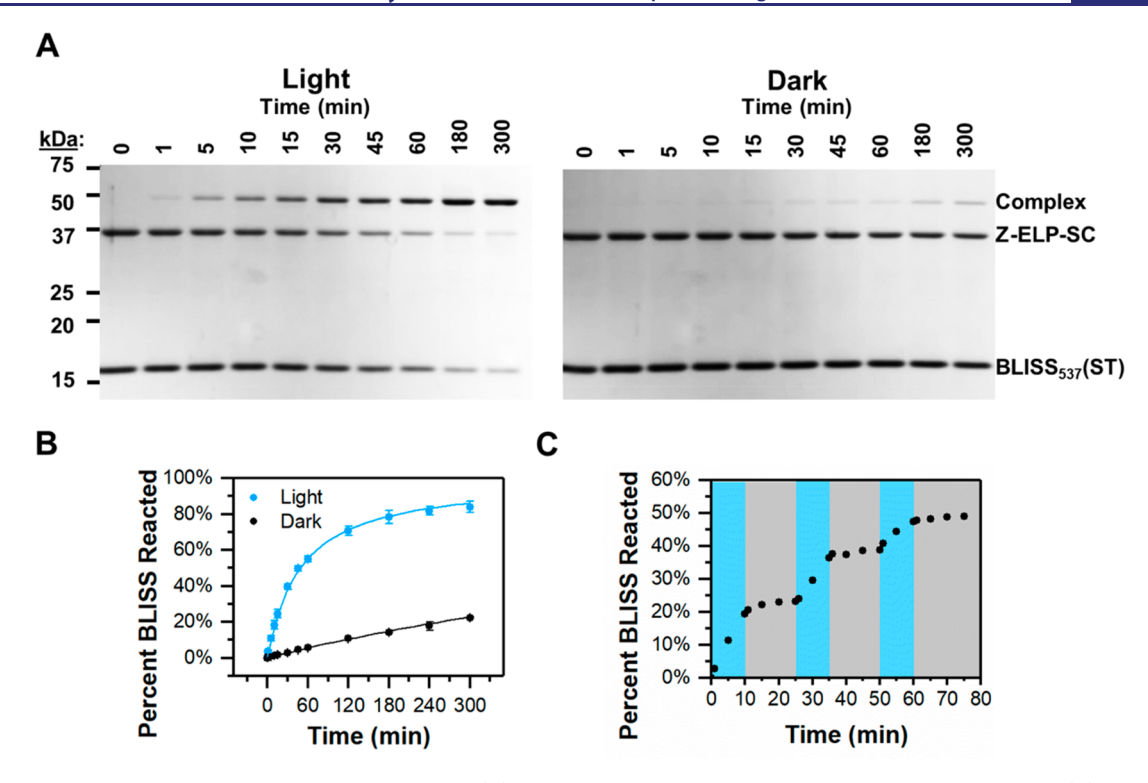


Figure 3. Time course studies for $BLISS_{537}ST$ reacting to SC. (A) Coomassie stained SDS-PAGEs of light and dark reactions. (B) The SDS-PAGE gels were analyzed via densitometry to calculate the percent $BLISS_{537}(ST)$ reacted at each time point. The average of three replicates is presented along with the standard deviation in error bars. The fitted second order rate equation is plotted as the solid lines. (C) Light pulses show the $BLISS_{537}(ST)/SC$ reaction can be quickly quenched by removing light. Three 10 min light pulses were applied (blue) with consecutive recovery in the dark for 15 min (gray).

minimal reactivity in the light state (Figure 2A and S1A). The 537 insertion exhibited good switching and reactivity in the light state (52% reacted) with relatively low background (4.8% reacted) in the dark. While slightly higher activities were detected by reacting to SC2.1 (Figure 2B), the overall trend remained similar. An increase in reactivity was observed at 100 μ M while maintaining excellent blocking, indicating the window of switching is in a higher micromolar range (Figure S2A and S2B).

While higher reactivity was observed for all BLISS(ST002) variants (Figures 2C and 2D and S1C and S1D), only variant 540 showed a high level of switching. Variants 541 and 544 exhibited no apparent blocking, and lowering the concentration did not dramatically change the switching behavior (Figure S2C and S2D), indicating there may be sequence related violations preventing the J α -helix from docking in the dark state.

We next performed time course studies for the $BLISS_{537}(ST)$ variant at fixed equimolar concentrations to determine the second order rate constants for the light and dark reactions (Figure 3). SDS-PAGE samples were taken over 5 h and analyzed using densitometry (Figure 3A). The reactions reached 84% completion in the light and only 22% in the dark. The extent of reaction was used to fit a second order rate model (Table S1). The second order rate equation model fit the data well, with R^2 values of 0.99 for the light and dark data (Figure 3B).

The light-responsive nature of AsLOV2 provides the opportunity to reversibly modulate the SpyCatcher/SpyTag reaction by blue light. This possibility was examined using BLISS₅₃₇(ST) with SC by irradiating with 10 min light pulses followed by 15 min of quenching in the dark (Figure 3C).

Upon removal of light, the reaction rate quickly flattened within seconds, and the reaction resumed with no delay upon light exposure. This observation is in good agreement with the fast photocycle half-life of the AsLOV2 on the order of seconds.³¹ The ability to turn on-and-off bioconjugation instantaneously using light allows precise spatial and temporal control of protein immobilization as well as labeling at the cellular level.

The ON reaction kinetics for the other BLISS variants and SpyCatcher combinations were also evaluated (Table S1). Overall, switching from SC to SC2.1 increases the rate constants by twofold. There are no trends in reactivity for either SpyTag with an insertion site, which seems to indicate that the identity of the SpyTag residues in certain positions plays more of a role in dictating reaction rate; although, the extent of overlap with the original AsLOV2 sequence (Figure 1B) does not appear to make any difference. Compared to an unblocked ST-ELP control, the BLISS system is slower in the light state, showing the AsLOV2 does partially block binding even when the $J\alpha$ - helix is unfolded (Figure S3 and Table S1).

While trends in reactivity with insertion site are not apparent (Table S1), there are trends for the dynamic range. The ratio of light to dark rate constants increased the further the SpyTag is inserted into the J α -helix (Figure 4). This is consistent with other reports, where the longer truncations are less able to cage the peptide within the dark state.³² The insertions with the highest ratio are 537 followed by 540; although, BLISS₅₄₀(ST002) has a similar ratio to BLISS₅₃₇(ST). While the reactivity is lower, the ST version exhibits better switching than SpyTag002.

Using the rate constants, we simulated the dark and light state switchability of three highest switching variants over a

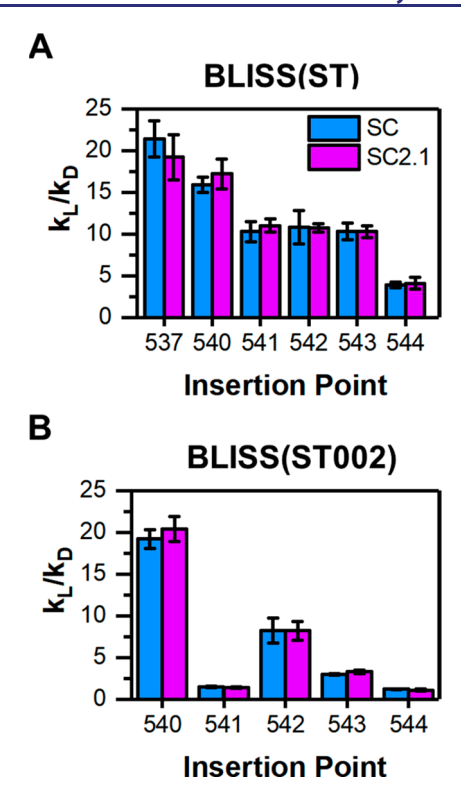


Figure 4. Ratio of light to dark rate constants for BLISS variants reacting to SC and SC2.1. The bars show the average percent BLISS reacted with the standard deviation from three replicates shown as error bars. (A) BLISS(ST) variant rate constant ratios. (B) BLISS(ST002) variant rate constant ratios.

range of concentrations (Figure S34). BLISS $_{537}(ST)$ offers the highest differences within the $10-100~\mu\mathrm{M}$ range (Figure S34C), making it useful for many applications. Faster reaction at low micromolar concentrations is possible using SC2.1 (Figure S34D), and the BLISS $_{540}(ST002)$ switches at even lower micromolar concentrations (Figure S34E and S34F). The slowest variant, BLISS $_{540}(ST)$, exhibits the highest switching above the micromolar range (Figure S34A and S4B) and is useful to achieve a small degree of conjugation without background.

We next demonstrated the use of BLISS₅₃₇(ST) for spatial control of protein conjugation onto a solid surface though photopatterning. We bound BLISS₅₃₇(ST) to nickel-coated glass slides, where 20 mm diameter well silicone isolators were adhered to the surface to contain the liquid in both the BLISS binding step and SpyCatcher exposure step. For a mask, three strips of 2-3 mm wide, opaque, black electrical tape were adhered to the other side of the slide. After BLISS₅₃₇(ST) binding, the surface was washed and exposed to mRuby2-SC and blue light for 5 min. Slides were washed and scanned (Figure 5A). The striped photomask was clearly defined, demonstrating precise spatial control over protein conjugation. A corresponding line profile of the slide also demonstrated highly specific, light-activated mRuby conjugation with low background in the dark region (Figure S5A). The low background mRuby2 signal is consistent with the low-level quantified from a similar nickel-coated 96-well plate (Figure

Sequential protein patterning onto the same surface was demonstrated using GFP-SC as our second fluorescent protein. A diagonally stripped mask was adhered to first conjugate

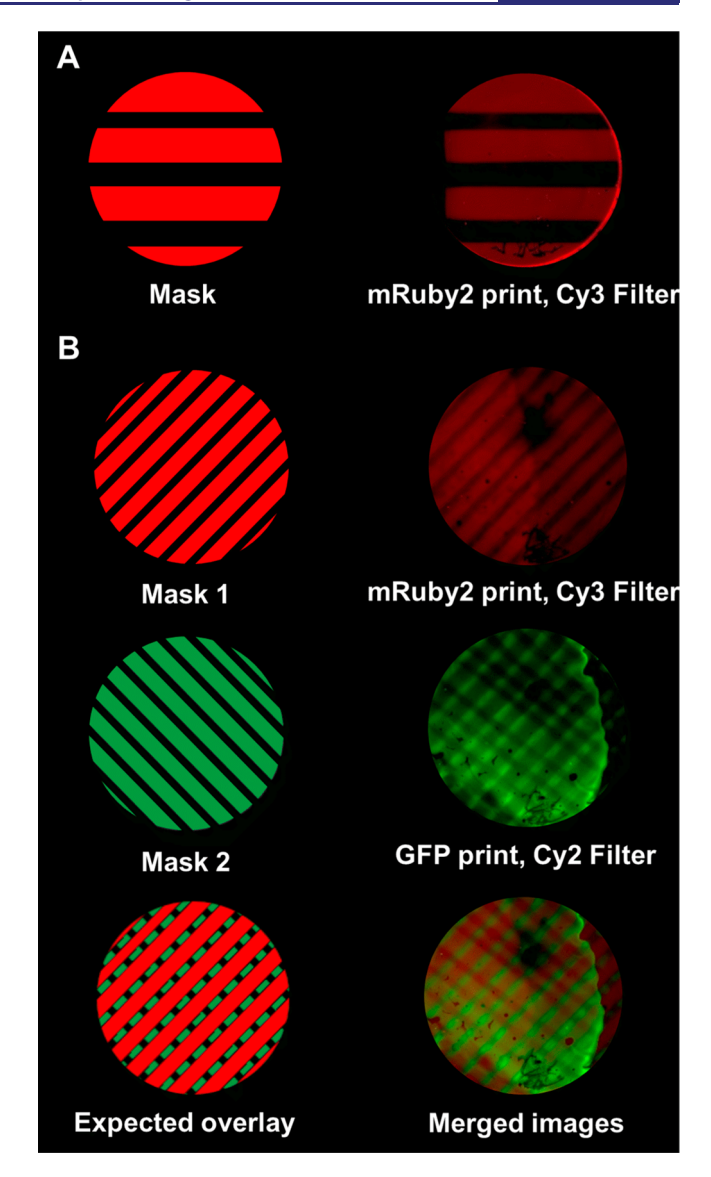


Figure 5. Photopatterned nickel coated slides. The wells are 20 mm in diameter. (A) Scan of photopatterned stripes of mRuby2-SC on a nickel coated glass slide. The slide was exposed to 5 μ M of mRuby2-SC for 5 min. (B) mRuby2 and GFP were sequentially printed onto glass slides, creating red and green perpendicular stripes. The Cy3 filter detects the red mRuby2 stripes, while the Cy2 filter detects the green GFP stripes. An overlay of the two shows a cross-hatched pattern.

mRuby2-SC (Figure 5B). While defined mRuby2 stripes were still observed, the overall patterning has less resolution and a higher background (Figure S5B). This is likely due to higher light deflection through the thinner stripes using our current light source. After washing, the mask was rotated 90° before being exposed to GFP-SC to print GFP stripes perpendicular to the mRuby2 stripes. Defined GFP patterns were detected primarily at areas where the green and red stripes did not overlap (Figure 5B and S5B). Only a low level of GFP was detected at sites that were already patterned with mRuby2, suggesting most BLISS proteins have already been conjugated with mRuby2 (Figure S5B). Collectively, these data demonstrate good spatial and temporal control of protein patterning.

In conclusion, we developed the first photoactivated SpyCatcher/SpyTag bioconjugation system, BLISS, where

the AsLOV2 photoreceptor was used to provide spatiotemporal control over intermolecular isopeptide bond formation. Both the original SpyTag and SpyTag002 could be inserted into the J α -helix and undergo light-dependent switching. The insertion location dictated both the dynamic range of the BLISS variant as well as the concentration ranges in which the switching could be observed. The further upstream locations provided the greatest ratio between light and dark kinetics, while the residue identity within certain positions influenced the reaction rate. The kinetics could be further shifted by swapping the SpyCatcher partner. Consistent with the fast photoresponsive nature of the LOV2 domain, the BLISS strategy offers instantaneous switching in SpyCatcher/SpyTag conjugation between the light and dark state. This exquisite switchability allows precision photopatterning of two fluorescent proteins onto a surface in a spatially controlled manner.

While we demonstrated the BLISS strategy only for *in vitro* biofabrication purposes, the capability of genetically encoding both conjugation components would enable the potential use for intracellular optogenetics applications. Unlike the majority of optogenetic tool sets, particularly in the blue light wavelengths, which quickly revert in the dark, the ability to form a stable attachment could expand the applications of using light for localization tracking and other genetic circuits.

ASSOCIATED CONTENT

Supporting Information

The Supporting Information is available free of charge at https://pubs.acs.org/doi/10.1021/jacs.1c03198.

Supplemental methods, table of oligos used, table of rate constants, amino acid sequences, and additional data (PDF)

AUTHOR INFORMATION

Corresponding Author

Wilfred Chen – Department of Chemical and Biomolecular Engineering, University of Delaware, Newark, Delaware 19716, United States; ⊚ orcid.org/0000-0002-6386-6958; Email: wilfred@udel.edu

Authors

Emily J. Hartzell – Department of Chemical and Biomolecular Engineering, University of Delaware, Newark, Delaware 19716, United States

Justin Terr – Department of Chemical and Biomolecular Engineering, University of Delaware, Newark, Delaware 19716, United States

Complete contact information is available at: https://pubs.acs.org/10.1021/jacs.1c03198

Author Contributions

The manuscript was written through contributions of E.J.H. and W.C. Experimental work was performed by E.J.H. and J.T. All authors have given approval to the final version of the manuscript.

Funding

This work was funded by grants from the NSF (DMR1609621, CBE1803008, and CBE1911950)

Notes

The authors declare no competing financial interest.

ACKNOWLEDGMENTS

We thank Brian Kuhlman for sharing plasmid pQE-80L iLID (C530M) (Addgene plasmid #60408) and Mark Howarth for sharing plasmid SpyDock (Addgene plasmid #124618).

ABBREVIATIONS

BLISS, blue light inducible spytag system; AsLOV2, *Avena sativa* light oxygen voltage domain 2; iLID, improved light inducible dimer; ST, SpyTag; ST002, SpyTag002; SC, SpyCatcher($\Delta N_1 \Delta C_2$); SC2.1, SpyCatcher2.1; ELP, elastin-like polypeptide; GFP, green fluorescent protein

REFERENCES

- (1) Keeble, A. H.; Howarth, M. Power to the Protein: Enhancing and Combining Activities Using the Spy Toolbox. *Chem. Sci.* **2020**, *11* (28), 7281–7291.
- (2) Reddington, S. C.; Howarth, M. Secrets of a Covalent Interaction for Biomaterials and Biotechnology: SpyTag and SpyCatcher. *Curr. Opin. Chem. Biol.* **2015**, *29*, 94–99.
- (3) Zakeri, B.; Fierer, J. O.; Celik, E.; Chittock, E. C.; Schwarz-Linek, U.; Moy, V. T.; Howarth, M. Peptide Tag Forming a Rapid Covalent Bond to a Protein, through Engineering a Bacterial Adhesin. *Proc. Natl. Acad. Sci. U. S. A.* **2012**, *109* (12), E690–697.
- (4) Levary, D. A.; Parthasarathy, R.; Boder, E. T.; Ackerman, M. E.; Najbauer, J. Protein-Protein Fusion Catalyzed by Sortase A. *PLoS One* **2011**, *6* (4), e18342.
- (5) Kim, H.; Siu, K. H.; Raeeszadeh-Sarmazdeh, M.; Sun, Q.; Chen, Q.; Chen, W. Bioengineering Strategies to Generate Artificial Protein Complexes. *Biotechnol. Bioeng.* **2015**, *112* (8), 1495–1505.
- (6) Shah, N. H.; Muir, T. W. Inteins: Nature's Gift to Protein Chemists. Chem. Sci. 2014, 5 (2), 446–461.
- (7) Keeble, A. H.; Banerjee, A.; Ferla, M. P.; Reddington, S. C.; Anuar, I. N. A. K.; Howarth, M. Evolving Accelerated Amidation by SpyTag/SpyCatcher to Analyze Membrane Dynamics. *Angew. Chem.* **2017**, *129* (52), *16748*–*16752*.
- (8) Keeble, A. H.; Turkki, P.; Stokes, S.; Khairil Anuar, I. N. A.; Rahikainen, R.; Hytonen, V. P.; Howarth, M. Approaching Infinite Affinity through Engineering of Peptide-Protein Interaction. *Proc. Natl. Acad. Sci. U. S. A.* **2019**, *116* (52), 26523–26533.
- (9) Ziegler, T.; Moglich, A. Photoreceptor Engineering. Front. Mol. Biosci. 2015, 2, 30.
- (10) Burdick, J. A.; Murphy, W. L. Moving from Static to Dynamic Complexity in Hydrogel Design. *Nat. Commun.* **2012**, 3 (1), 1269.
- (11) Ruskowitz, E. R.; DeForest, C. A. Photoresponsive Biomaterials for Targeted Drug Delivery and 4D Cell Culture. *Nat. Rev. Mater.* **2018**, 3 (2), 17087.
- (12) Ronzitti, E.; Emiliani, V.; Papagiakoumou, E. Methods for Three-Dimensional All-Optical Manipulation of Neural Circuits. *Front. Cell. Neurosci.* **2018**, *12*, 469.
- (13) Fairbanks, B. D.; Scott, T. F.; Kloxin, C. J.; Anseth, K. S.; Bowman, C. N. Thiol-Yne Photopolymerizations: Novel Mechanism, Kinetics, and Step-Growth Formation of Highly Cross-Linked Networks. *Macromolecules* **2009**, *42* (1), 211–217.
- (14) Fairbanks, B. D.; Schwartz, M. P.; Halevi, A. E.; Nuttelman, C. R.; Bowman, C. N.; Anseth, K. S. A Versatile Synthetic Extracellular Matrix Mimic via Thiol-Norbornene Photopolymerization. *Adv. Mater.* **2009**, *21* (48), 5005–5010.
- (15) Kloxin, A. M.; Kasko, A. M.; Salinas, C. N.; Anseth, K. S. Photodegradable Hydrogels for Dynamic Tuning of Physical and Chemical Properties. *Science* **2009**, 324 (5923), 59–63.
- (16) DeForest, C. A.; Polizzotti, B. D.; Anseth, K. S. Sequential Click Reactions for Synthesizing and Patterning Three-Dimensional Cell Microenvironments. *Nat. Mater.* **2009**, *8* (8), 659–664.
- (17) DeForest, C. A.; Anseth, K. S. Cytocompatible Click-Based Hydrogels with Dynamically Tunable Properties through Orthogonal Photoconjugation and Photocleavage Reactions. *Nat. Chem.* **2011**, 3 (12), 925–931.

- (18) Wu, X.; Huang, W.; Wu, W.-H.; Xue, B.; Xiang, D.; Li, Y.; Qin, M.; Sun, F.; Wang, W.; Zhang, W.-B.; Cao, Y. Reversible Hydrogels with Tunable Mechanical Properties for Optically Controlling Cell Migration. *Nano Res.* **2018**, *11* (10), 5556–5565.
- (19) Horner, M.; Raute, K.; Hummel, B.; Madl, J.; Creusen, G.; Thomas, O. S.; Christen, E. H.; Hotz, N.; Gubeli, R. J.; Engesser, R.; Rebmann, B.; Lauer, J.; Rolauffs, B.; Timmer, J.; Schamel, W. W. A.; Pruszak, J.; Romer, W.; Zurbriggen, M. D.; Friedrich, C.; Walther, A.; Minguet, S.; Sawarkar, R.; Weber, W. Phytochrome-Based Extracellular Matrix with Reversibly Tunable Mechanical Properties. *Adv. Mater.* **2019**, *31* (12), 1806727.
- (20) Xiang, D. F.; Wu, X.; Cao, W.; Xue, B.; Qin, M.; Cao, Y.; Wang, W. Hydrogels With Tunable Mechanical Properties Based on Photocleavable Proteins. *Front. Chem.* **2020**, *8*, 7.
- (21) Wang, R.; Yang, Z.; Luo, J.; Hsing, I. M.; Sun, F. B₁₂-Dependent Photoresponsive Protein Hydrogels for Controlled Stem Cell/Protein Release. *Proc. Natl. Acad. Sci. U. S. A.* **2017**, *114* (23), 5912–5917.
- (22) Lyu, S.; Fang, J.; Duan, T.; Fu, L.; Liu, J.; Li, H. Optically Controlled Reversible Protein Hydrogels Based on Photoswitchable Fluorescent Protein Dronpa. *Chem. Commun.* **2017**, *53* (100), 13375–13378.
- (23) Zhang, X.; Dong, C.; Huang, W.; Wang, H.; Wang, L.; Ding, D.; Zhou, H.; Long, J.; Wang, T.; Yang, Z. Rational Design of a Photo-Responsive UVR8-Derived Protein and a Self-Assembling Peptide—Protein Conjugate for Responsive Hydrogel Formation. *Nanoscale* **2015**, 7 (40), 16666–16670.
- (24) Jia, H.; Kai, L.; Heymann, M.; García-Soriano, D. A.; Härtel, T.; Schwille, P. Light-Induced Printing of Protein Structures on Membranes in Vitro. *Nano Lett.* **2018**, *18* (11), 7133–7140.
- (25) Hammer, J. A.; Ruta, A.; West, J. L. Using Tools from Optogenetics to Create Light-Responsive Biomaterials: LOVTRAP-PEG Hydrogels for Dynamic Peptide Immobilization. *Ann. Biomed. Eng.* **2020**, 48 (7), 1885–1894.
- (26) Beyer, H. M.; Thomas, O. S.; Riegel, N.; Zurbriggen, M. D.; Weber, W.; Hörner, M. Generic and Reversible Opto-Trapping of Biomolecules. *Acta Biomater.* **2018**, *79*, 276–282.
- (27) Shadish, J. A.; Strange, A. C.; DeForest, C. A. Genetically Encoded Photocleavable Linkers for Patterned Protein Release from Biomaterials. *J. Am. Chem. Soc.* **2019**, *141* (39), 15619–15625.
- (28) Wong, S.; Mosabbir, A. A.; Truong, K.; Isalan, M. E. An Engineered Split Intein for Photoactivated Protein Trans-Splicing. *PLoS One* **2015**, *10* (8), e0135965.
- (29) Tyszkiewicz, A. B.; Muir, T. W. Activation of Protein Splicing with Light in Yeast. *Nat. Methods* **2008**, *5* (4), 303–305.
- (30) Hoffmann, M. D.; Bubeck, F.; Eils, R.; Niopek, D. Controlling Cells with Light and LOV. *Adv. Biosyst.* **2018**, 2 (9), 1800098.
- (31) Zimmerman, S. P.; Kuhlman, B.; Yumerefendi, H. Engineering and Application of LOV2-Based Photoswitches. *Methods Enzymol.* **2016**, *580*, 169–190.
- (32) Strickland, D.; Lin, Y.; Wagner, E.; Hope, C. M.; Zayner, J.; Antoniou, C.; Sosnick, T. R.; Weiss, E. L.; Glotzer, M. TULIPs: Tunable, Light-Controlled Interacting Protein Tags for Cell Biology. *Nat. Methods* **2012**, *9* (4), 379–384.
- (33) Mart, R. J.; Meah, D.; Allemann, R. K. Photocontrolled Exposure of Pro-apoptotic Peptide Sequences in LOV Proteins Modulates Bcl-2 Family Interactions. *ChemBioChem* **2016**, *17* (8), 698–701.
- (34) Guntas, G.; Hallett, R. A.; Zimmerman, S. P.; Williams, T.; Yumerefendi, H.; Bear, J. E.; Kuhlman, B. Engineering an Improved Light-Induced Dimer (iLID) for Controlling the Localization and Activity of Signaling Proteins. *Proc. Natl. Acad. Sci. U. S. A.* **2015**, *112* (1), 112–117.
- (35) Lungu, O. I.; Hallett, R. A.; Choi, E. J.; Aiken, M. J.; Hahn, K. M.; Kuhlman, B. Designing Photoswitchable Peptides Using the AsLOV2 Domain. *Chem. Biol.* **2012**, *19* (4), 507–517.
- (36) Niopek, D.; Benzinger, D.; Roensch, J.; Draebing, T.; Wehler, P.; Eils, R.; Di Ventura, B. Engineering Light-Inducible Nuclear

- Localization Signals for Precise Spatiotemporal Control of Protein Dynamics in Living Cells. *Nat. Commun.* **2014**, *5*, 4404.
- (37) Li, L.; Fierer, J.; Rapoport, T.; Howarth, M. Structural Analysis and Optimization of the Covalent Association between SpyCatcher and a Peptide Tag. *J. Mol. Biol.* **2014**, *426* (2), 309–317.
- (38) Khairil Anuar, I. N. A.; Banerjee, A.; Keeble, A. H.; Carella, A.; Nikov, G. I.; Howarth, M. Spy&Go Purification of SpyTag-Proteins using Pseudo-SpyCatcher to Access an Oligomerization Toolbox. *Nat. Commun.* **2019**, *10* (1), 1734.
- (39) Swartz, A. R.; Chen, W. SpyTag/SpyCatcher Functionalization of E2 Nanocages with Stimuli Responsive Z-ELP Affinity Domains for Tunable Monoclonal Antibody Binding and Precipitation Properties. *Bioconjugate Chem.* **2018**, 29 (9), 3113–3120.
- (40) Sun, Q.; Chen, Q.; Blackstock, D.; Chen, W. Post-Translational Modification of Bio-Nanoparticles as a Modular Platform for Biosensor Assembly. ACS Nano 2015, 9 (8), 8554–8561.